Acta Geodyn. Geomater., Vol. 3, No. 3 (143), 23-29, 2006

PRELIMINARY RESULTS OF THE ANALYSIS OF THE GPS TIME SERIES SOLUTIONS (GPSSTS) IN ASG-PL PERMANENT NETWORK

Władysław GÓRAL* and Daniel JASIURKOWSKI

AGH University of Science and Technology (AGH-UST), Faculty of Mining Surveying and Environmental Engineering, al. Mickiewicza 30, 30-059 Krakow, Poland
**Corresponding author's e-mail*: wgik@agh.edu.pl

(*Received* February 2006, *accepted* June 2006)

ABSTRACT
The permanent GPS stations are particulary important for studying various phenomena because they provide uninterrupted measurements allowing to form the time series of station coordinates. Analysis of GPS solutions time series (GPSSTS) for short meridian baselines were explored in the paper (Kryński and Zanimonskiy, 2000). In our article we intend to extend the analysis of the GPSSTS for baselines of different lengths and azimuths. GPS observation data from the ASG-PL network have been used in the research. The GPSSTS in time and frequecy domain have been analyzed. The spectrums of the GPSSTS with the using coherence function were compared. Moreover, a practical approach to correct any unmodeled effects in GPS baseline solutions that cannot be computed using classical GPS adjustment was presented.

KEYWORDS: permanent GPS stations, time series, GPS data processing

1. INTRODUCTION

Currently, in the south of Poland, there are nine operating permanent GPS stations: WROC (Wroclaw), KATO (Katowice), ZYWI (Zywiec), WODZ (Wodzisław Śląski), TARG (Tarnowskie Góry), KLOB (Klobuck), LELO (Lelów), KRAW (Krakow), SACZ (Nowy Sacz), (status: January 2006). These stations are included in the ASG-PL network. They operate continuously delivering observations to the Data Center in Katowice (www.asg-pl.pl). The network covers entire area of Upper Silesian Coal Basin in Poland and forms precise reference frame for geodetic and geodynamic applications. The activity of the stations mentioned also stimulates researches on accuracy improvement, reliability and efficiency of positioning using the GPS permanent stations. In the article (Kryński and Zanimonskiy, 2000) there was explored the GPSSTS for short meridian baselines. In this article we explored the GPSSTS for different lengths and azimuths baselines from ASG-PL network. We analyzed the GPSSTS using their different visualizations, forms and domain to find any regularities which could be used to practical improving baseline solutions inside the network area.

2. EXPLORING DATA AND THEIR PREPARATION

In this article, we used GPS observation data from seven permanent stations: KATO, KLOB, LELO, TARG, WODZ, ZYWI and KRAW. The maximum difference between elevations of these stations is 145 m. Their equipment was homogeneous. Every sample of the GPSSTS is the solution of chosen baseline for a 3-hour session which was shifted every 30 min. The solutions of baselines were computed in the Lc mode (Yong-Hui at al., 2004), with a elevation cut-off angle established at 12^o. In Fig. 1a, the draft of the explored network is plotted. In Fig. 1b, the draft of the studied baselines, placed according to their directions, is plotted. In Fig. 1b, we translated all the baselines into one common point. To compute the baseline solutions we used the broadcast and precise ephemeris. In this manner, during a week time, we were able to generate the 337 samples of the GPSSTS.

In Table 1, there are the characteristics of generated GPSSTS. Some of the chosen sessions were not resolved, so we had breaks in the GPSSTS. This feature is showed in Tab.1 by the parameter called average efficiency, which is computed as a percentage rate of the number of solutions we reached to the number of all computed sessions. Because the spectral analysis we used in this research required equidistant sampling data, we completed these places in the GPSSTS. To eliminate impulse noise in the GPSSTS we used a median smoothing filter (Stranneby, 2004).

3. THE RESEARCH METHODOLOGY AND THE RESULTS

3.1. ANALYSIS IN THE TIME DOMAIN

In Fig. 2, an example of the GPSSTS for baselines with similar directions and reverse azimuth is shown. We can point out that the demonstrated GPSSTS are almost symmetrical. This feature is

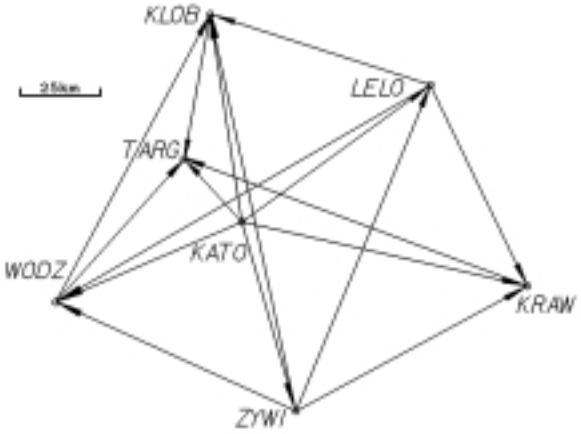

Fig. 1a The draft of the network of the studied baselines.

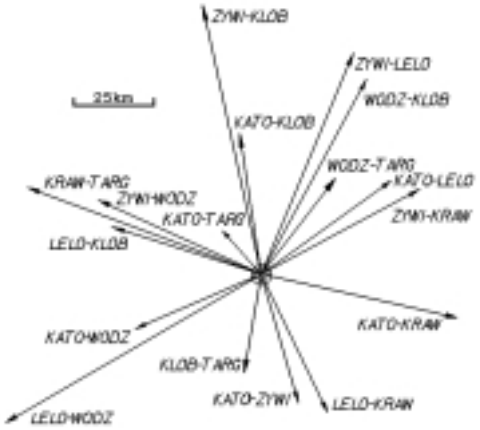

Fig. 1b Draft of the studied baselines sorted according to their directions.

Table 1 Characteristics of generated GPSSTS for every computing span.

Computing span	all computed sessions	average number of solutions for broadcast eph.	average number of solutions for precise eph.	average efficiency for broadcast eph. [%]	average efficiency for precise eph. [%]
172-178 DOY 2004	343	330	332	96.5	96.7
284-296 DOY 2004	583	562	567	96.4	97.3
079-099 DOY 2005	1015	1005	1006	99.0	99.1
177-201 DOY 2005	1207	1191	1191	98.7	98.7

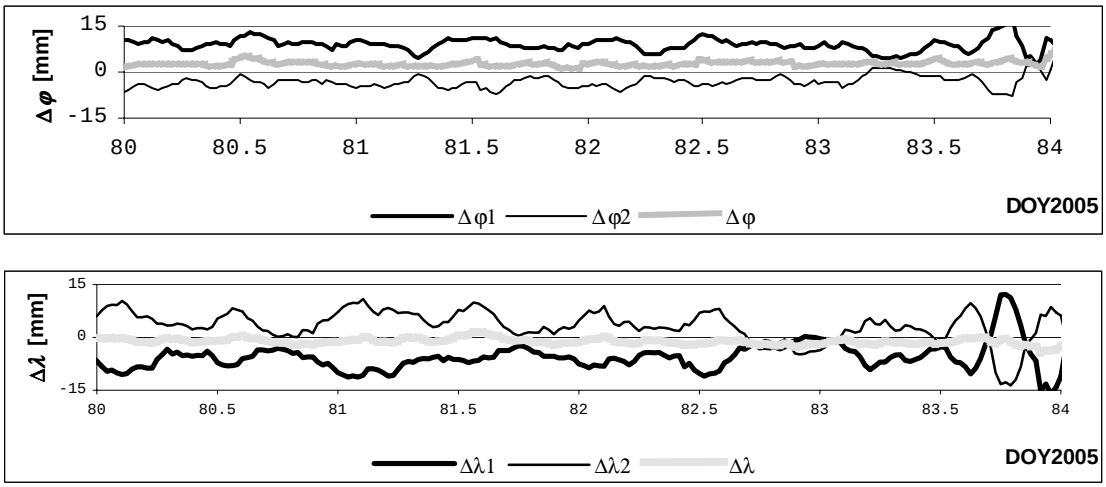

Fig. 2 The GPSSTS ($\Delta\varphi_1$, $\Delta\lambda_1$) for KATO-KRAW baseline; ($\Delta\varphi_2$, $\Delta\lambda_2$) for KRAW-TARG baseline and their averages – ($\Delta\varphi$, $\Delta\lambda$), interval 80-84 DOY2005, precise ephemeris.

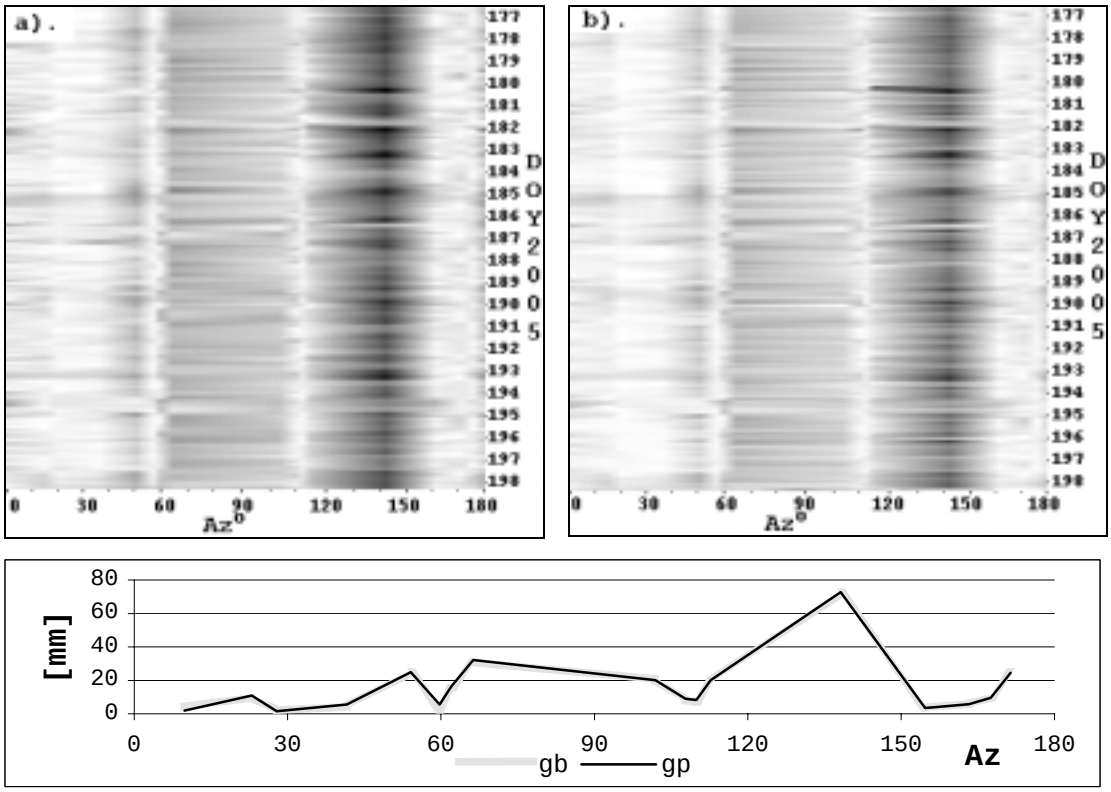

Fig. 3 The time series of baselines horizontal component errors in azimuth function, interval 177-198 DOY2005 (for 3a and 3b values are increasing with darkness).

common in most of the cases and indicates some dependence between the baseline solution and its azimuth. Residuals: $\Delta\varphi(t_i)$, $\Delta\lambda(t_i)$, $\Delta h(t_i)$ were expressed in [mm] as:

$$\begin{aligned}\Delta\varphi(t_i) &= R(\varphi_o - \varphi(t_i)) \\ \Delta\lambda(t_i) &= R(\lambda_o - \lambda(t_i))\cos\varphi_o \\ \Delta h(t_i) &= h_o - h(t_i)\end{aligned} \quad (1)$$

where R – mean Earth radius, φ_o, λ_o, h_o – geodetic coordinates (precise), $\varphi(t_i)$, $\lambda(t_i)$, $h(t_i)$ – geodetic coordinates (computed). To simplify the writing we assumed that: $\Delta\varphi = \Delta\varphi(t_i)$, $\Delta\lambda = \Delta\lambda(t_i)$, $\Delta h = \Delta h(t_i)$.

Taking into account the symmetric feature presented in Fig. 2 we tried to analyze the GPSSTS depending on their azimuths. In order to present the GPSSTS for the purpose of more density spread arguments, we made the direction reductions of baselines from the third and fourth quarter of the reference frame to the first and second quarter. To reach this goal we used the rule that, if a reduced baseline is changing its azimuth up to 180°, its GPSSTS are changing signs. To eliminate the dependence of GPSSTS on lengths of the baselines we scaled the time series and multiplied them with a K factor (2). In this manner we reduced every GPSSTS to one of 100 km baseline (see e.g.: Kostelecký, 2002). The reductions described above are expressed as:

$$\Delta\varphi_z = \begin{cases} K\Delta\varphi, & Az \in (0^0, 180^0\rangle \\ -K\Delta\varphi, & Az \in (180^0, 360^0\rangle \end{cases},$$

$$\Delta\lambda_z = \begin{cases} K\Delta\lambda, & Az \in (0^0, 180^0\rangle \\ -K\Delta\lambda, & Az \in (180^0, 360^0\rangle \end{cases},$$

$$\Delta h_z = \begin{cases} K\Delta h, & Az \in (0^0, 180^0\rangle \\ -K\Delta h, & Az \in (180^0, 360^0\rangle \end{cases}, \quad K = \frac{100\,\mathrm{km}}{d}, \quad (2)$$

where d is the length of the baseline in kilometers. In Fig. 3a, the dependence time series of errors of horizontal baseline components in (reduced) azimuth functions for broadcast ephemeris: $g_b = \sqrt{\Delta\varphi_{zb}{}^2 + \Delta\lambda_{zb}{}^2}$ are presented, in turn in Fig. 3b, the same time series generated with using precise ephemeris: $g_p = \sqrt{\Delta\varphi_{zp}{}^2 + \Delta\lambda_{zp}{}^2}$ are presented. In Fig. 3c, the average values from Fig 3a and 3b: $\overline{g_b} = E(g_b)$ and $\overline{g_p} = E(g_p)$ are showed.

In Figs. 3a and 3b, in the neighborhood of azimuth 140°, we can see a dark vertical stripe. It indicates that the baselines which have an azimuth of about 140° have the largest errors. In the

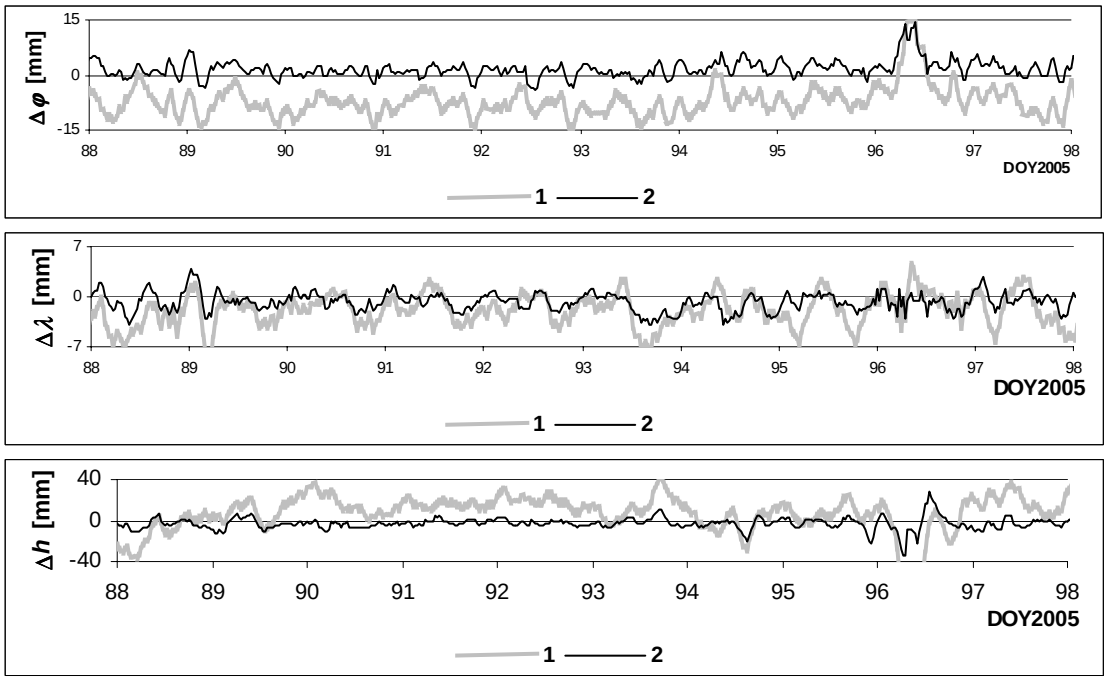

Fig. 4 The GPSSTS of $\Delta\varphi$, $\Delta\lambda$ and Δh of WODZ-TARG baseline before correcting (1) and after correcting (2), interval 88-98 DOY2005, precise ephemeris.

neighborhood of azimuth 30°, we can see solutions with the lowest errors. Comparing Figs. 3a and 3b we can see that they have similar distribution for both kinds of ephemeris. This is confirmed in Fig. 3c.

3.2. THE CORRECTING OF THE BASELINE SOLUTIONS INSIDE THE AREA OF THE PERMANENT STATION NETWORK

For the marking point, which is inside the permanent network, there is the possibility to compute the corrections for solution of marking point GPS baseline, which was computed using firmware software. In order to reach this goal, we had to compute the coordinates of the marking point, which is referenced to one of the three permanent station triangle vertexes. This task, we carried out with an example of marking point T(TARG), referenced to permanent stations: K(KATO), L(LELO), W(WODZ) (Fig. 1). For any example session we have to compute baselines: W-K, L-W, K-W. Comparing the computed coordinates with their precise values we obtained residuals: $\Delta\varphi_K$, $\Delta\varphi_W$, $\Delta\varphi_L$, $\Delta\lambda_K$, $\Delta\lambda_W$, $\Delta\lambda_L$, Δh_K, Δh_W, Δh_L. Following this, we put the obtained residuals into three sets of equations:

$$\begin{cases} \Delta\varphi_K = \alpha_\varphi(\varphi_K - \varphi_W) + \beta_\varphi(\lambda_K - \lambda_W) \\ \Delta\varphi_W = \alpha_\varphi(\varphi_W - \varphi_L) + \beta_\varphi(\lambda_W - \lambda_L) \\ \Delta\varphi_L = \alpha_\varphi(\varphi_W - \varphi_K) + \beta_\varphi(\lambda_L - \lambda_K) \end{cases},$$

$$\begin{cases} \Delta\lambda_K = \alpha_\lambda(\varphi_K - \varphi_W) + \beta_\lambda(\lambda_K - \lambda_W) \\ \Delta\lambda_W = \alpha_\lambda(\varphi_W - \varphi_L) + \beta_\lambda(\lambda_W - \lambda_L) \\ \Delta\lambda_L = \alpha_\lambda(\varphi_W - \varphi_K) + \beta_\lambda(\lambda_L - \lambda_K) \end{cases},$$

$$\begin{cases} \Delta h_K = \alpha_h(\varphi_K - \varphi_W) + \beta_h(\lambda_K - \lambda_W) \\ \Delta h_W = \alpha_h(\varphi_W - \varphi_L) + \beta_h(\lambda_W - \lambda_L) \\ \Delta h_L = \alpha_h(\varphi_W - \varphi_K) + \beta_h(\lambda_L - \lambda_K) \end{cases}. \quad (3)$$

The solution of sets of equations (3) results in the three pairs of parameters: (α_φ, β_φ), (α_λ, β_λ), (α_h, β_h) which are usable to compute the corrections for the coordinates of the unknown station TARG from, for example, the baseline WODZ-TARG according to formulas:

$$\begin{aligned} \Delta\varphi_T &= \alpha_\varphi(\varphi_T - \varphi_W) + \beta_\varphi(\lambda_T - \lambda_W) \\ \Delta\lambda_T &= \alpha_\lambda(\varphi_T - \varphi_W) + \beta_\lambda(\lambda_T - \lambda_W) \\ \Delta h_T &= \alpha_h(\varphi_T - \varphi_W) + \beta_h(\lambda_T - \lambda_W) \end{aligned} \quad (4)$$

After correcting the coordinates of station TARG we reached an even 70% better station marking, for both of the used ephemeris. This method is especially effective for correcting of the elevation (Góral W., 2004). In Fig. 4, the GPSSTS of WODZ-TARG before and after correcting are showed. We can see that the amplitude of the GPSSTS after corrections is much lower. In Fig. 5, the plot of parameters α_φ, β_φ, α_λ, β_λ, α_h and β_h is given.

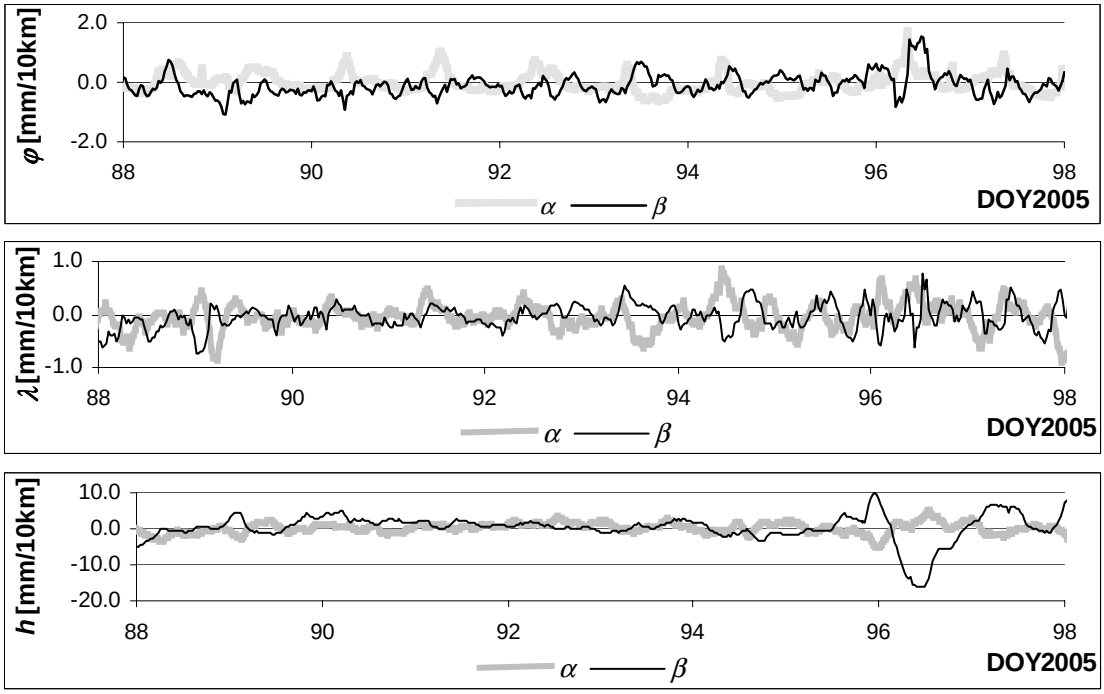

Fig. 5 The time series of parameters α_φ, β_φ, α_λ, β_λ, α_h and β_h.

3.3. ANALYSIS IN THE FREQUENCY DOMAIN

In order to find the regularity of the analyzed time series in the frequency domain, we researched their spectrums with the Blackman-Tukey method based on the Fourier transform of auto-covariance and cross-covariance function of analyzed time series (Kosek, 2001; Strangely, 2004). The spectral analysis demonstrated that there is no dominate harmonic component in the GPSSTS. In that situation, we decided to research the differences of the GPSSTS generated using broadcast and precise ephemeris and to explore similarities between spectrums of the GPSSTS.

In Fig. 6, an example of visualization of time series power spectrum of differences between the GPSSTS generated with using broadcast and precise ephemeris is shown. This plot is presented in function of azimuths and lengths of baselines according to formulas:

$$m(Az,CPW)=\sqrt{\left\|F(\Delta\varphi_b-\Delta\varphi_p)\right\|^2+\left\|F(\Delta\lambda_b-\Delta\lambda_p)\right\|^2} \tag{5a}$$

$$m(d,CPW)=\sqrt{\left\|F(\Delta\varphi_b-\Delta\varphi_p)\right\|^2+\left\|F(\Delta\lambda_b-\Delta\lambda_p)\right\|^2} \tag{5b}$$

Where F indicates a transform of the time series and $\|\ \|$ is a module of complex number. Every value of the spectrum is expressed in the CPW – cycles per week function. In order to stress the dominant harmonic component in the type (5a) time series, for every baseline, we introduced a method of spectrum scaling expressed by the formula:

$$m(Az,CPW)_s = \\ = m(Az,CPW)\frac{\max[m(Az,CPW)]-\min[m(Az,CPW)]}{\max[m(Az)]-\min[m(Az)]} \tag{6}$$

The method of scaling spectrum, introduced in formula (6), moves the maximum values of each GPSSTS to a maximum value of all of the GPSSTS. The minimum values were traced in similar way like the maximum values. In Fig. 6c, three examples of type (5a) time series for baselines whose azimuths are: 6^o, 29^o and 175^o (true: 6^o, 29^o and 355^o) were presented. They are profiles of Fig. 6a. In turn, in Fig. 6d, three examples of type (5a) time series for baselines whose lengths are: 25 km, 106 km and 137 km were presented. They are profiles of Fig. 6b.

In the time series of the differences between the GPSSTS generated using broadcast and precise ephemeris, we found sharp harmonic components. In Fig. 6a there is a stressed stripe of maximum values of baseline spectrums for the day period. We can issue half-day periods too, but they are lower stressed. Therefore, the differences between solutions using precise ephemeris and broadcast ephemeris, are the day and half-day harmonic components. In Fig. 6b we can see that the detected harmonic components are stronger for longer baselines.

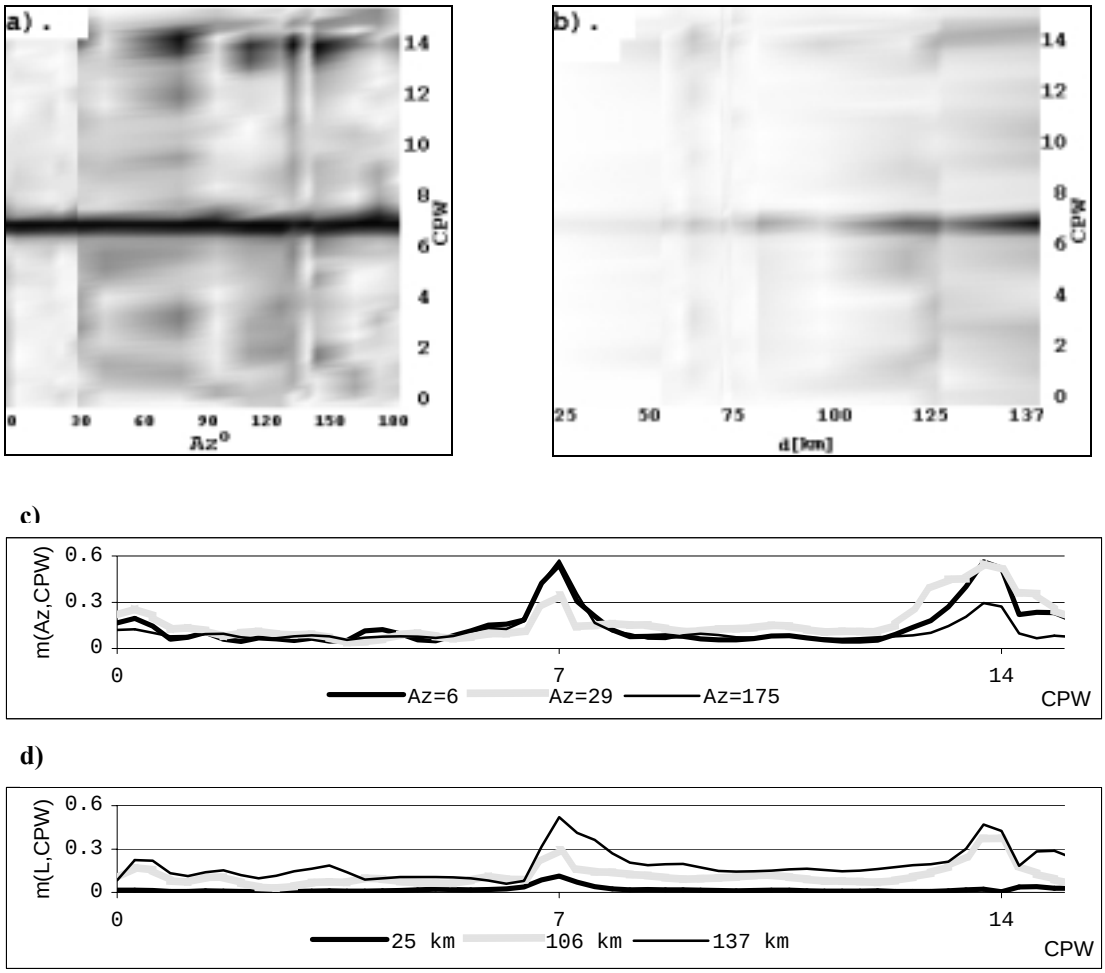

Fig. 6 The spectrum power of differences between the GPSSTS generated using broadcast and precise ephemeris in azimuths and lengths function, interval 177-201 DOY2005, (for 6a and 6b values are increasing with darkness).

In order to compare the spectrums of the GPSSTS we used coherency function (Popiński and Kosek, 2000; Kosek, 2001). Comparisons showed that the time series of a similar azimuth baselines have a similar spectrums for that horizontal component of position, which is less important for the computation of the length of baselines. For prime vertical baselines it is the λ component, for meridian baselines it is the φ component. For baselines whose reduced azimuth is near to 45^o or 135^o, the coherence function is casual. The spectra are similar for are similar for both of the used ephemeris. In Figs. 7a and 7b, the examples of coherency function for GPSSTS, respectively, almost prime vertical and almost meridian baselines, are presented.

4. CONCLUSIONS

In this article we looked for the regularities in local GPS permanent network by researching the GPSSTS of this network. Our results partially confirmed existing regularities in baseline solutions. However, we frequently found these regularities not directly in the GPSSTS but in some performing forms of the GPSSTS or special ways of presenting them. This is the result of GPS adjustment implemented in software generating the GPSSTS. This software efficiently eliminates systematic factors from baselines solution. We showed that some combinations of the GPSSTS like time series of differences between the GPSSTS generated using broadcast and precise ephemeris or spectrum comparison functions, lead us to find residual factors which are not included in GPS adjusting. Therefore, we can ask if there is any sense in constructing models. Correction for baseline solutions based on such parameters like baseline azimuth, length and location can be modeled. Besides models of atmospheric refraction we should also develop empirical models.

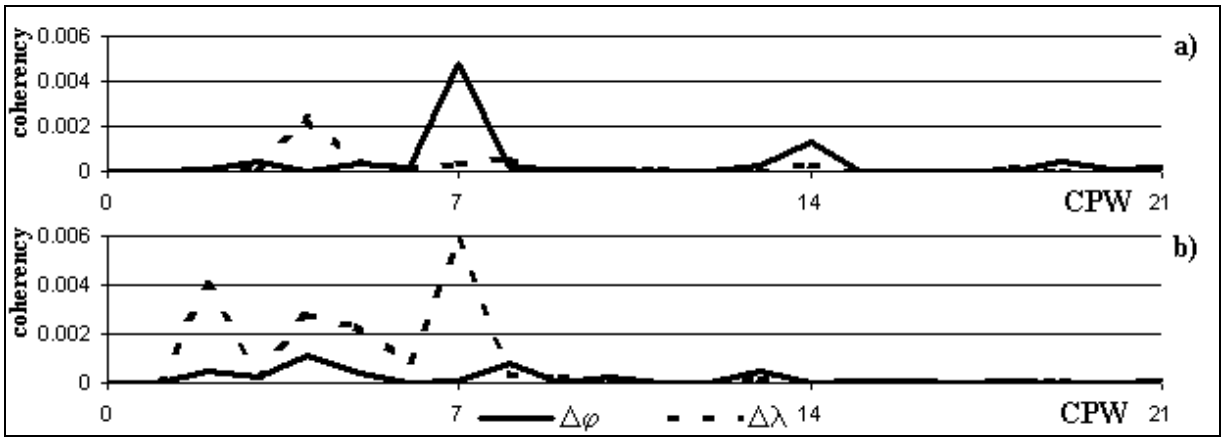

Fig. 7 The coherency of the GPSSTS of $\Delta\varphi$ and $\Delta\lambda$, interval 172-178 DOY2004, precise ephemeris.

ACKNOWLEDGEMENT

The research has been supported by the AGH-UST in Krakow in frame of the project No.11.11.150.478.

REFERENCES

Góral, W.: 2005, Badawcza sieć geodynamiczna na obszarze wschodniej części Górnośląskiego Zagłębia Węglowego (in Polish with English summ.), UWND-AGH, Kraków.

Kosek, W.: 2001, Metody analiz widmowych, filtracji i prognozowania, CBK-PAN, Warszawa, http://www.cbk.waw.pl/~kosek

Kostelecký, J.: 2002, On the use of permanent GPS stations in geodynamics, ACTA MONTANA IRSM AS CR, Series A, No. 20 (124), 45-49.

Kryński, J. and Zanimonskiy, Y.M.: 2000, Analiza zmienności w ciągach rozwiązań GPS i ciągach obserwacji grawimetrycznych (in Polish with English summ.), IGiK, Serie monograficzne, Warszawa.

Popiński, W. and Kosek, W.: 2000, Comparison of various spectro-temporal coherence functions between polar motion and atmospheric excitation functions, Artificial Satelites, Vol. 35, No. 4, Warszawa.

Stranneby, D.: 2004, Digital signal processing: DSP and applications by Dag Stranneby (in Polish), BTC, Warszawa.

Yong-Hui, L., Kyung-Chul, Y., Dong-Rak, Y. and Jung-Soo, H.: 2004, Baseline analysis about linear combination using GPS data, GNSS-UNSW, Busan – Płd. Korea, http://www.gmat.unsw.edu.au/gnss2004unsw/HONG,%20Jung-Soo%20P59.pdf